Michigan State University

National Superconducting Cyclotron Laboratory

MULTIFRAGMENT EMISSION IN THE REACTION $^{36}Ar + ^{197}Au$ at E/A = 35, 50, 80, AND 110 MeV

R.T. de SOUZA, L. PHAIR, D.R. BOWMAN, N. CARLIN, C.K. GELBKE, W.G. GONG, Y.D. KIM, M.A. LISA, W.G. LYNCH, G.F. PEASLEE, M.B. TSANG, H.M. XU, F. ZHU, and W.A. FRIEDMAN

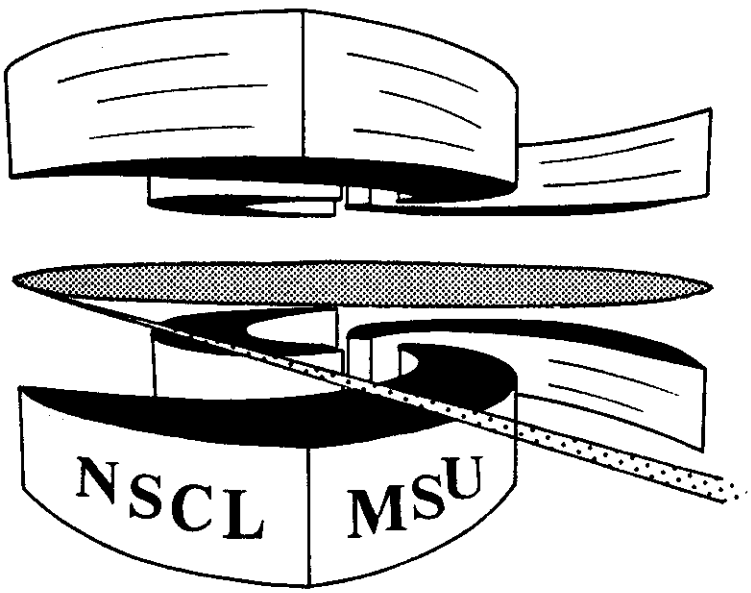

MSUCL-785

JUNE 1991

MSUCL-785
June, 1991

Multifragment Emission In the Reaction $^{36}Ar + ^{197}Au$ at E/A = 35, 50, 80, and 110 MeV

R.T. de Souza, L. Phair, D.R. Bowman, N. Carlin*, C.K. Gelbke, W.G. Gong, Y.D. Kim, M.A. Lisa, W.G. Lynch, G.F. Peaslee, M.B. Tsang, H.M. Xu, and F. Zhu
National Superconducting Cyclotron Laboratory
and Department of Physics and Astronomy
Michigan State Universlty, East Lansing, MI 48824

W.A. Friedman
Department of Physics, University of Wisconsin, Madlson, WI 53706

Abstract

Multifragment emission in the reaction $^{36}Ar + ^{197}Au$ at E/A=35, 50, 80, and 110 MeV has been measured with a low-threshold 4π detector array. Over this broad range of incident energies, the mean values and variances of the Intermediate mass fragment (IMF: $3 \leq Z \leq 20$) multiplicity distributions exhibit an approximate scaling with the total charged particle multiplicity. The measured multiplicities of light particles and intermediate mass fragments are compared with both a model involvIng statistical decay of an expandlng compound nucleus, and with a model involving microscopic quasi-particle dynamics. The statistical decay model predictions are sensltive to the low-density nuclear equation of state.

---

* Present address: Instituto de Fisica, Universldade de São Paulo, C. Postal 20516, CEP 01498, São Paulo, Brazil

Under extreme conditions of temperature and pressure, nuclear matter may preferentially decay by multifragment emission [1-6]. Such a decay mode would represent a new and interesting phenomenon. Many mechanisms have been proposed [1-14] for the production of the fragments. For example, the action of thermal pressure may force hot, nuclear systems to expand to low density where the exponential growth of density fluctuations may lead to a complete disintegration of the nuclear system [1,4]. Unfortunately, detailed comparisons of various fragment production models to experimental data have been lacking since few experiments [15-20] performed to date provided sufficient phase space coverage to allow the extraction of exclusive quantities. To address this question of multifragment decay of highly excited nuclear systems and to provide constraints for various theoretical models, we have measured both total charged particle and intermediate mass fragment (IMF: $3 \leq Z \leq 20$) multiplicities for the $^{36}Ar + ^{197}Au$ reaction at E/A = 35, 50, 80, and 110 MeV.

The experiment was performed at the National Superconducting Cyclotron Laboratory of Michigan State University where ^{36}Ar beams of E/A = 35, 50, 80, and 110 MeV accelerated by the K1200 cyclotron bombarded a 1 mg/cm^2 ^{197}Au target. Reaction products of a nuclear collision were detected with the Miniball [21], a low-threshold 4π detector array covering polar angles of $9^\circ \leq \theta \leq 160^\circ$ with a geometric efficiency of 89% of 4π. The measurements at E/A=35 MeV were performed with reduced angular coverage, $16^\circ \leq \theta \leq 160^\circ$. Quasi-elastic projectile-like fragments as well as heavy residues emitted at more forward angles were not detected. Reaction products were identified by atomic number for $Z \approx 1$-20 with representative detection thresholds of E/A=2, 3, and 4 MeV for Z=3, 10, and 18 fragments, respectively.

A qualitative perspective of the evolution of the reaction with increasing bombarding energy is provided by Fig. 1. In this figure, the correlation between the total detected charge, Z_{sum}, of all particles ($Z \lesssim 25$) and the total charged particle multiplicity, N_C, is presented. At each bombarding energy, the total detected charge increases with increasing multiplicity as the collisions evolve from peripheral to central. At the lowest energy, E/A=35 MeV, the charged particle multiplicities are relatively small and only a small fraction of the nuclear system is observed as light particles and intermediate mass fragments. This observation is consistent with the survival of heavy reaction residues which are not identified in the present experiment and therefore not included in Z_{sum}. As the bombarding energy per nucleon is increased to 50, 80 and finally 110 MeV, one observes a correlated increase in both the total charged particle multiplicity and the total detected charge. The multiplicity associated with central collisions increases from $N_C \approx 11$ at E/A=35 MeV to $N_C \approx 30$ at E/A=110 MeV. The average total detected charge for central collisions increases from 22% of the total charge of the system at E/A=35 MeV to 61% at E/A=110 MeV, where a number of events were observed for which more than 80% of the total charge of the system was detected. These latter events correspond to a nearly complete disintegration of the system into light particles and intermediate mass fragments.

To better characterize the various classes of multifragment events, we have extracted the probability distributions $P(N_{IMF})$ of detecting N_{IMF} intermediate mass fragments in a single collision for different gates on the charged particle multiplicity N_C. The four panels in Fig. 2 depict these distributions. At each energy, the IMF multiplicity distributions become wider

and shift towards higher average multiplicities as the charged particle multiplicity increases. Peripheral reactions, selected by $N_C \lesssim 7$, exhibit narrow IMF multiplicity distributions peaked at $N_{IMF}=0$. For these collisions, IMF emission is an unlikely process. On the other hand, for central collisions, selected by large values of N_C, IMF emission is a common process for which the average IMF multiplicity increases from $\langle N_{IMF}\rangle \approx 1$ at E/A=35 MeV to $\langle N_{IMF}\rangle \approx 4$ at E/A=110 MeV. At the highest incident energy, events are observed in which more than 10 intermediate mass fragments are detected in the exit channel.

To allow quantitative comparisons of IMF multiplicity distributions, we have determined their first and second moments, $\langle N_{IMF}\rangle$ and σ^2_{IMF}. The dependence of these moments on the total charged particle multiplicity N_C is shown in Fig. 3. Values extracted at different incident energies are shown by different symbols as indicated by the key in the figure. At all energies, $\langle N_{IMF}\rangle$ and σ^2_{IMF} exhibit an initial, approximately linear increase as a function of N_C. The slope of this increase is rather similar for the four energies investigated. For large values of N_C, corresponding to the extreme tails of the respective N_C distributions, both $\langle N_{IMF}\rangle$ and σ^2_{IMF} increase only marginally as a function of N_C.

The relationship between the IMF and total charged particle multiplicities can be qualitatively understood by assuming that the charged particle multiplicity is strongly correlated with energy deposition and that the production of intermediate mass fragments depends primarily upon this energy deposition. The nearly universal increase of $\langle N_{IMF}\rangle$ as a function of N_C can thus be viewed as due to the selection of interactions involving a progressively increasing

amount of internal energy deposition. For orientation, the upper panel of Fig. 3 includes an approximate scale of the relation between the excitation energy of the emitting system and the mean charged particle multiplicity calculated from the statistical model of ref. [6]. In the extreme tails of the N_C distributions, the correlation between internal energy and N_C becomes dominated by fluctuations of the charged particle multiplicity. Hence, very large values of N_C become ineffective in selecting nuclei of increasing internal energy thus causing the observed saturation of $\langle N_{IMF} \rangle$ and σ^2_{IMF} at large values of N_C.

We have compared the experimentally measured IMF multiplicity distributions with the predictions of the decay model discussed in ref. 6. This schematic model couples the phase-space features of statistical decay with the dynamical features of expansion. It has the capacity for predicting both multiplicity distributions of species of particles (IMF's in particular) and their spectra. The model has been successfully employed [22] to interpret the low emission temperatures deduced from the relative population of states [23], as well as the trends in IMF multiplicity with excitation energy [17] where the multiplicity is found and predicted to be less than one [24]. It also predicted [6] a sharp rise in multiplicity for excitation energies on the order of 8 MeV/nucleon. The calculations require an assumption of initial source mass, charge, and thermal excitation energy when the system is at normal density. For simplicity we assumed the decaying source to be the full composite system (A=233, Z=97), and we further assumed that the system expanded with no initial expansion velocity from normal density. While varying the excitation energy we noted the correlation between the predicted total charged particle multiplicity and the features of the predicted IMF multiplicity distributions.

The model ignores angular momentum, fluctuations in source size and excitation energy, and the lack of thermal equilibrium. While the inclusion of such effects might affect the final observations, we nonetheless find that the essential features of the observed data are included in the predictions of the schematic model shown by the curves in Fig. 3. The sensitivity to the source size was explored by changing the initial mass and charge by 20%. The qualitative conclusions remain valid despite this change.

The calculations are sensitive to the assumption of nuclear compressibility at low density. The solid, dashed, and dashed-dotted curves in Fig. 3 show predictions for the relationship between the mean IMF and charged particle multiplicities for finite-nucleus compressibilities of K=144, 200, and 288 MeV, respectively [25]. IMF multiplicities for a non-expanding compound nucleus, corresponding to the limit $K \to \infty$, are shown by the dashed-dotted-dotted curves. To illustrate instrumental distortions, the dotted curves show the calculations for K=200 MeV, filtered by the response of the experimental apparatus; such distortions are too small to affect the qualitative conclusions of this paper. At low multiplicities, corresponding to low excitation in this model, the nucleus does not expand and all calculations predict IMF multiplicities consistent with the measured values. For multiplicities larger than $N_C \approx 20$, however, the expansion strongly influences the predicted number of clusters in the final state. Large observed IMF multiplicities comparable to the measured values are only predicted for an equation of state that is sufficiently soft to allow the nucleus to expand in response to thermal pressure. Very stiff low-density equations of state hinder the expansion of the system leading to a suppression of the production of multifragment final states and a

consequent underprediction of the observed mean IMF multiplicities by a factor of two.

The calculations with the schematic model suggest that multifragment decays of highly excited nuclear systems may exhibit considerable sensitivity to the low-density nuclear equation of state. They indicate that the expansion dynamics, which is governed by this property, may be intimately connected to the production of IMFs. A more quantitative exploration of these properties, however, will require a more complete model.

We have also performed calculations with the microscopic quasi-particle dynamics (QPD) model of ref. [11]. In collisions leading to a total multiplicity of 36-45, these calculations predict average multiplicities of significantly less than one for fragments with $3 \leq Z \leq 20$ and, in addition, the formation of a single heavy residue. These predicted IMF multiplicities are much smaller than those observed experimentally.

In summary, we have studied multifragment emission in $^{36}Ar+^{197}Au$ reactions over a broad range of incident energies. The mean values and variances of the multiplicity distributions of intermediate mass fragments were found to increase as a function of the total charged particle multiplicity which may be interpreted as a rough measure for the internal energy of the fragment emitting system. An average multiplicity of 4 intermediate mass fragments is observed for the most central collisions at E/A=110 MeV. These large IMF multiplicities are consistent with predictions of a statistical model for

evaporation from an expanding compound nucleus, provided that a soft low-density equation of state is employed. Calculations with the quasi-particle dynamics model of ref. [11] predict too low fragment multiplicities.

We gratefully acknowledge fruitful discussions with D.H. Boal and his permission to use the QPD program of ref. [11]. This work is based upon work supported by the National Science Foundation under Grant numbers PHY-86-11210, PHY-89-13815, and PHY-90-15255. W.G. Lynch acknowledges the receipt of a U.S. Presidential Young Investigator Award and N. Carlin acknowledges partial support by the FAPESP, Brazil.

References

1. G. Bertsch and P.J. Siemens, Phys. Lett. 126B (1983) 9.
2. L.P. Cernai and J. Kapusta, Phys. Reports 131 (1986) 223.
3. W. Lynch, Ann. Rev. Nucl. Part. Sci. 37 (1987) 493, and refs. therein.
4. T.J. Schlagel and V.R. Pandharipande, Phys. Rev. C36 (1987) 162.
5. D.H.E. Gross, Rep. Prog. Phys. 53 (1990) 605, and refs. therein.
6. W.A. Friedman, Phys. Rev. C42 (1990) 667.
7. L.G. Moretto, Nucl. Phys. A247 (1975) 211.
8. W.A. Friedman and W.G. Lynch, Phys. Rev. C28 (1983) 16; C28 (1983) 950.
9. W. Bauer et al., Phys. Rev. Lett. 58 (1987) 863.
10. G. Peilert et al., Phys. Rev. C39 (1989) 1402.
11. D.H. Boal and J.N. Glosli, Phys. Rev. C37 (1988) 91; C42 (1990) R502.
12. W. Bauer, et al., Phys. Lett. B150 (1985) 53, Nucl. Phys. A452 (986) 699.
13. T.S. Biro et al., Nucl. Phys. A459 (1986) 692.
14. C. Cerruti et al., Nucl. Phys. A476 (1988) 74.
15. K.G.R. Doss et al., Phys. Rev. Lett. 59 (1987) 2720.
16. R. Bougault, et al., Nucl. Phys. A488 (1988) 255c.
17. R. Trockel et al., Phys. Rev. C39 (1989) 729.
18. R. Bougault et al., Phys. Lett. B232 (1989) 291.
19. Y.D. Kim et al., Phys. Rev. Lett. 63 (1989) 494.
20. Y. Blumenfeld et al., Phys. Rev. Lett. 66 (1991) 576.
21. R.T. de Souza et al. Nucl. Instr. and Meth. A295 (1990) 109.
22. W.A. Friedman, Phys. Rev. Lett. 60 (1988) 2125.
23. Z. Chen et al., Phys. Rev. C36 (1987) 2297, and refs. therein.
24. W.A. Friedman, Phys. Rev. C40 (1989) 2055.
25. J.P. Blaizot, Phys. Reports 64 (1980) 171.

Figure Captions

Fig. 1: Measured relation between charged particle multiplicity, N_c, and total charge of identified particles ($Z \lesssim 25$) for the $^{40}Ar+^{197}Au$ reaction at the indicated energies. Correspondence between color and relative number of counts is: white (0-3), blue (4-9), green (10-27), yellow (28-81), red (82-243), and black (243-4000).

Fig. 2: Measured IMF multiplicity distributions for the indicated gates on charged particle multiplicity N_c. Panels are labeled by incident energy.

Fig. 3: First and second moments of IMF multiplicity distributions as a function of charged particle multiplicity, N_c. Different symbols represent results for indicated beam energies. The solid, dashed, dotted-dashed, and dashed-dotted-dotted curves show results calculated for the statistical decay of expanding compound nuclei of finite-nucleus compressibility K=144, 200, 288, and ∞, respectively. The dotted curves represent the calculations for K=200, filtered by the detector response.

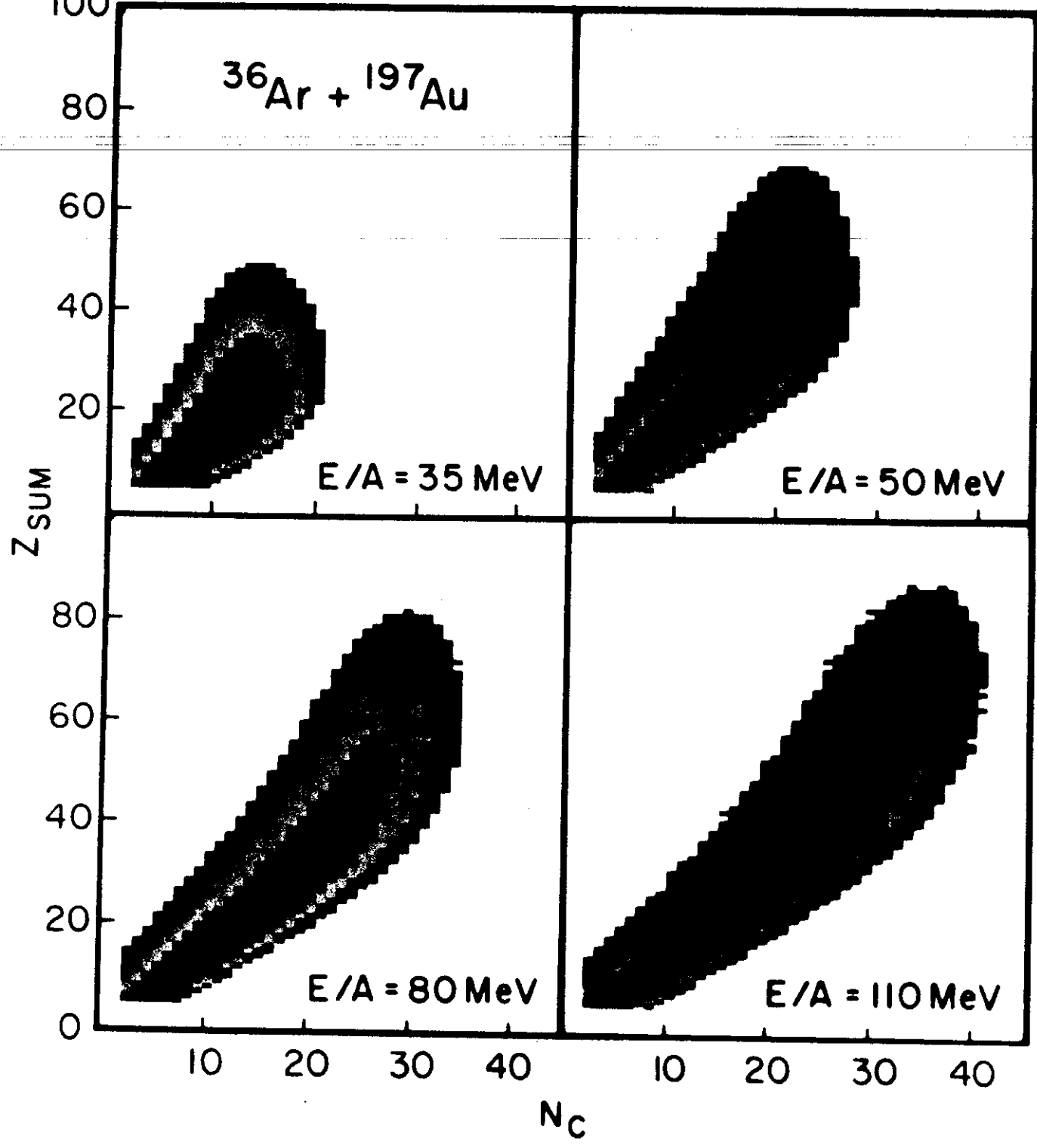
$^{36}Ar + ^{197}Au$
E/A = 35 MeV
E/A = 50 MeV
E/A = 80 MeV
E/A = 110 MeV
Z_{SUM}
N_C
0
20
40
60
80
100
10
20
30
40

Fig. 1

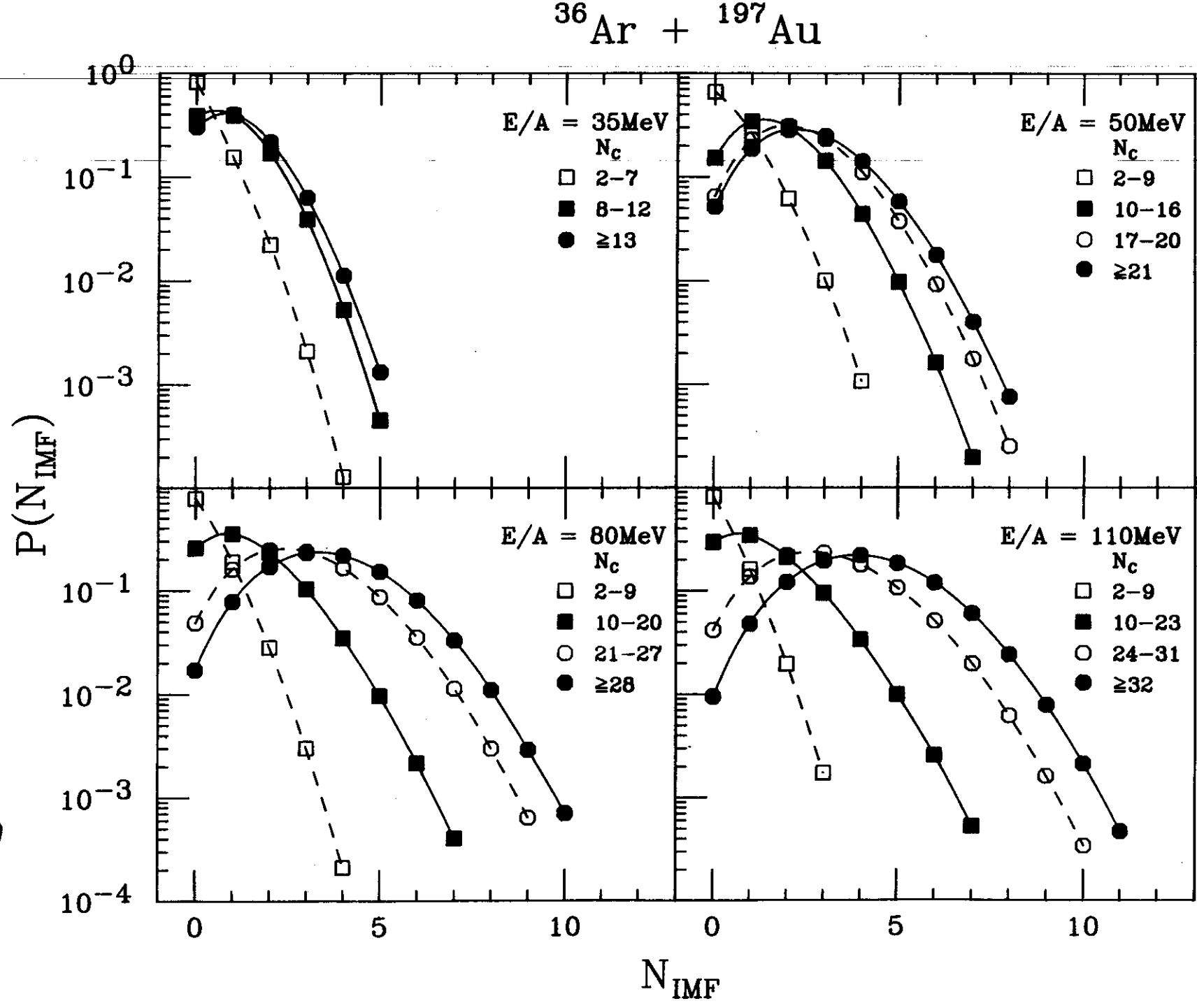
$^{36}Ar + ^{197}Au$
E/A = 35MeV
N_c
2–7
8–12
≥13
E/A = 50MeV
N_c
2–9
10–16
17–20
≥21
E/A = 80MeV
N_c
2–9
10–20
21–27
≥28
E/A = 110MeV
N_c
2–9
10–23
24–31
≥32
$P(N_{IMF})$
N_{IMF}
10^0
10^{-1}
10^{-2}
10^{-3}
10^{-4}
0
5
10

Fig. 2

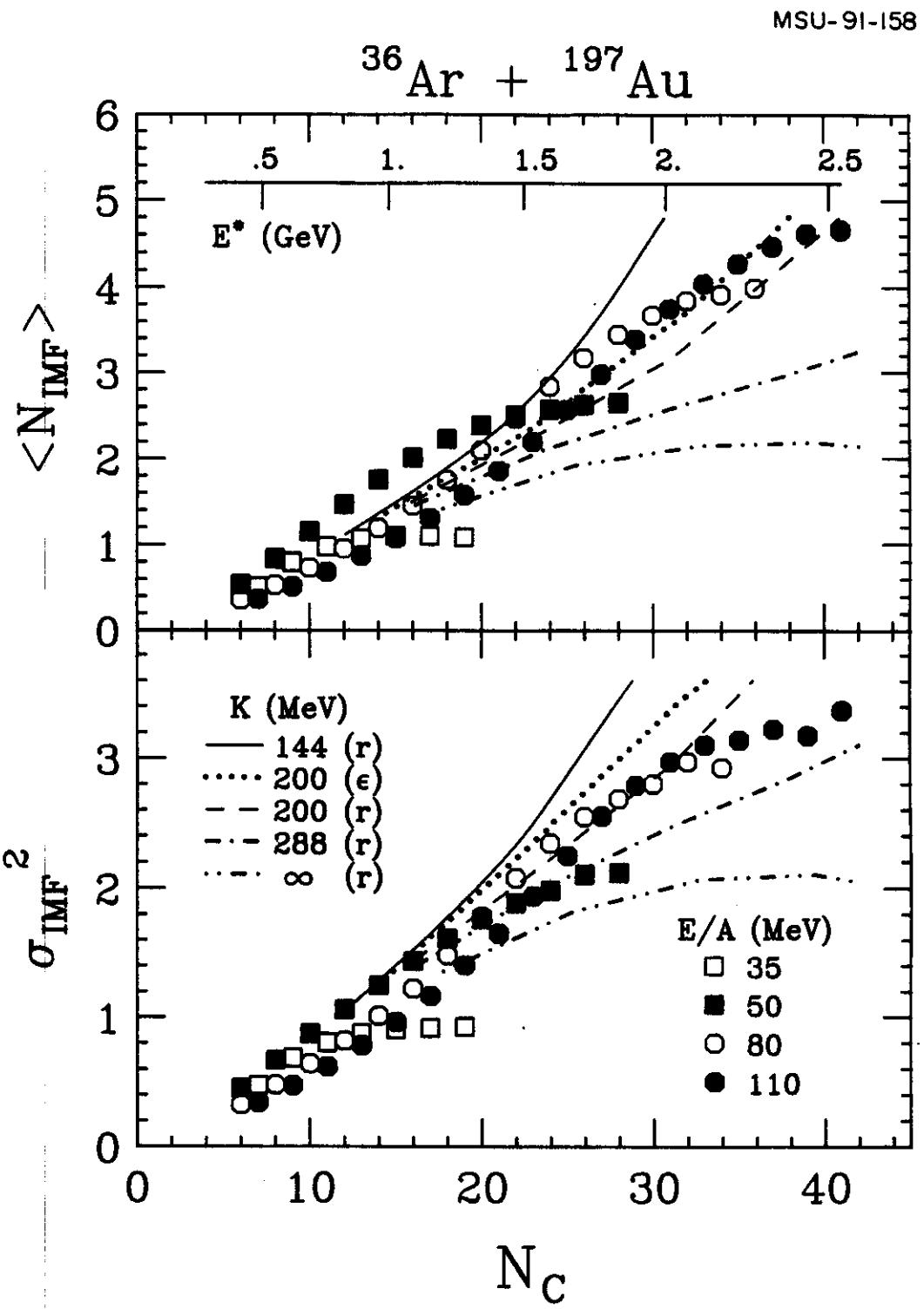
MSU-91-158
$^{36}Ar + ^{197}Au$
$\langle N_{IMF} \rangle$
E* (GeV)
.5
1.
1.5
2.
2.5
σ^2_{IMF}
K (MeV)
144 (r)
200 (ϵ)
200 (r)
288 (r)
∞ (r)
E/A (MeV)
35
50
80
110
N_C

Fig. 3